RNA polymerase approaches its promoter without long-range sliding along DNA

Larry J. Friedman, Jeffrey P. Mumm, and Jeff Gelles[1]

Department of Biochemistry, Brandeis University, Waltham, MA 02454

Edited* by Steven M. Block, Stanford University, Stanford, CA, and approved May 2, 2013 (received for review January 4, 2013)

Sequence-specific DNA binding proteins must quickly bind target sequences, despite the enormously larger amount of nontarget DNA present in cells. RNA polymerases (or associated general transcription factors) are hypothesized to reach promoter sequences by facilitated diffusion (FD). In FD, a protein first binds to nontarget DNA and then reaches the target by a 1D sliding search. We tested whether *Escherichia coli* σ^{54}RNA polymerase reaches a promoter by FD using the colocalization single-molecule spectroscopy (CoSMoS) multiwavelength fluorescence microscopy technique. Experiments directly compared the rates of initial polymerase binding to and dissociation from promoter and nonpromoter DNAs measured in the same sample under identical conditions. Binding to a nonpromoter DNA was much slower than binding to a promoter-containing DNA of the same length, indicating that the detected nonspecific binding events are not on the pathway to promoter binding. Truncating one of the DNA segments flanking the promoter to a length as short as 7 bp or lengthening it to ∼3,000 bp did not alter the promoter-specific binding rate. These results exclude FD over distances corresponding to the length of the promoter or longer from playing any significant role in accelerating promoter search. Instead, the data support a direct binding mechanism, in which σ^{54}RNA polymerase reaches the local vicinity of promoters by 3D diffusion through solution, and suggest that binding may be accelerated by atypical structural or dynamic features of promoter DNA. Direct binding explains how polymerase can quickly reach a promoter, despite occupancy of promoter-flanking DNA by bound proteins that would impede FD.

1D diffusion | total internal reflection fluorescence | transcription initiation

The binding of a multisubunit RNA polymerase (RNAP) or general transcription factors to a specialized transcription promoter DNA sequence is an essential step in initiating DNA transcription in all organisms (1, 2). Control of this promoter binding step is a key mechanism by which gene expression is regulated (3). To understand how this regulation occurs, it is necessary to understand the process by which the transcription machinery efficiently finds and binds to target sequences embedded in chromosomal DNA, where targets are outnumbered by orders of magnitude excess nontarget DNA.

Bacterial transcription is a convenient model system for studying promoter search, because the process can be efficiently reconstituted in vitro from purified components and bacterial RNAP holoenzymes recognize and bind directly to specific promoter DNA sequence motifs (4, 5). For the well-studied *Escherichia coli* RNAP, the rate at which the enzyme finds its cognate promoters can approach or even possibly exceed limits calculated for simple 3D diffusion of the protein up to the target sequence followed by direct promoter binding (6–8). Although there are uncertainties in calculating the magnitude of this limit because of uncertain contributions from orientation constraints and electrostatic steering (9), a long-standing view is that the rapid binding evades the rate limitation of pure 3D diffusion/direct binding by a facilitated diffusion (FD) process (10, 11). In FD, repeated instances of sequence nonspecific binding are followed by 1D sliding diffusion along the DNA in search of a specific binding site for the protein (Fig. 1*A*) (12). The involvement of 1D diffusion effectively creates a large target for binding that includes DNA segments flanking the promoter sequence and thus, accelerates the rate at which the protein finds the promoter.

Bacterial RNAP holoenzymes have multiple DNA binding domains that interact with different parts of the promoter sequence, and some of these domains are flexibly tethered (3, 5). The tethers make possible relative movement of the DNA binding domains over distances corresponding to a few tens of base pairs (3), a distance scale similar to the physical size of the promoter. Consequently, the mechanism and kinetics of forming specific RNAP–DNA contacts after RNAP closely (on the order of 10 nm or less) approaches promoter sequences are complex, and the process probably cannot be adequately understood in terms of either FD or 3D diffusion/binding models, both of which treat RNAP as a rigid body moving relative to the DNA. In contrast, these models are expected to be fully capable of describing the approach to the promoter from distances much larger than the physical size of the promoter.

For *E. coli* σ^{70}RNAP, there is some experimental evidence for an FD mechanism for promoter search over distances of 250 bp up to thousands of base pairs (refs. 13–21 and ref. 22 and references therein). However, the evidence is, in general, weak (*Discussion*) (9, 22, 23). Effective experimental tests have been complicated by (*i*) the general inability of bulk experiments to directly measure promoter binding uncoupled from subsequent conformational changes (2, 24) and (*ii*) the weak sequence specificity of DNA binding (25, 26).

In a previous study (7), we used colocalization single-molecule spectroscopy (CoSMoS) to directly observe and measure the initial rate of binding of σ^{54}RNAP to a cognate promoter uncoupled from subsequent conformational isomerization of the polymerase–promoter complex. We also showed that the initial RNAP–promoter complex that we observe is on the pathway to transcription initiation. σ^{54}RNAP also has the advantage relative to σ^{70}RNAP that promoter recognition may be more specific (27–29). Here, we extend the earlier approach; we measure binding and dissociation kinetics to both promoters and nonpromoter DNA and use these measurements to directly test the predictions of the FD model.

Results

Observed Nonspecific Binding Is Too Slow to Explain Promoter Binding Rates. We compared the rates of initial binding of σ^{54}RNAP holoenzyme to two different species of DNA: a *glnAp2* promoter-containing 853-bp DNA (called 598**P**255, because it contains 598 bp upstream and 255 bp downstream of the promoter;) and an 825-bp DNA (825**N**) that is essentially identical, except for the deletion of 27 bp containing the core promoter (Figs. S1 and S2). Rates of the binding step were measured using

Author contributions: L.J.F., J.P.M., and J.G. designed research; L.J.F. performed research; L.J.F. contributed new reagents/analytic tools; L.J.F. analyzed data; and L.J.F., J.P.M., and J.G. wrote the paper.

The authors declare no conflict of interest.

*This Direct Submission article had a prearranged editor.

[1]To whom correspondence should be addressed. E-mail: gelles@brandeis.edu.

This article contains supporting information online at www.pnas.org/lookup/suppl/doi:10.1073/pnas.1300221110/-/DCSupplemental.

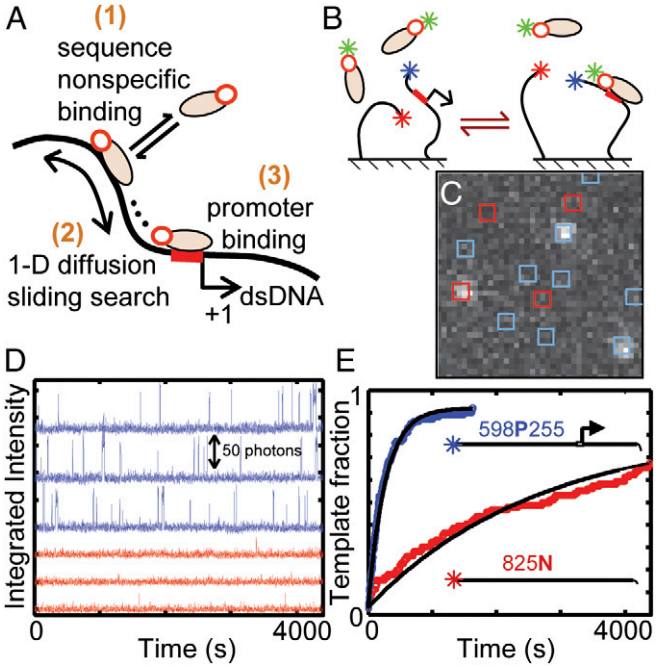

Fig. 1. Single-molecule test of the FD hypothesis for σ^{54}RNAP binding to a promoter. (*A*) Facilitated diffusion hypothesis for binding of RNAP holoenzyme (oval, core RNAP; circle, σ^{54} subunit) to DNA containing a cognate promoter (bent arrow). (*B*) Single-molecule experiment to compare the binding rate of σ^{54}RNAP labeled with Cy3 (green star) with a promoter (**P**) containing DNA 598**P**255 (labeled with Alexa Fluor 488; blue star) and a nonpromoter (**N**) DNA 825**N** (labeled with Cy5; red star). (*C*) Example image region (6 × 6 μm) showing spots of RNAP fluorescence (monochrome image) at locations of 598**P**255 molecules (blue squares) and 825**N** molecules (red squares). Total σ^{54}RNAP concentration is 0.1 nM. (*D*) Example records of σ^{54}RNAP fluorescence intensity recorded from 3 × 3-pixel squares (as in *C*) centered at the positions of three 598**P**255 molecules (blue) and three 825**N** molecules (red). (*E*) Fraction of DNA molecules that bound RNAP at least one time before the indicated time (blue and red) and exponential fits (black) yielding apparent first-order rate constants [blue: $(3.7 \pm 0.5) \times 10^{-3}$ s^{-1}, N_D = 102 DNA molecules; red: $(0.4 \pm 0.1) \times 10^{-3}$ s^{-1}, N_D = 96]. A control experiment (Fig. S4) showed that binding rate was independent of the dye that was used to label the DNA.

a modification of the CoSMoS method that was described previously (7). The two kinds of DNA molecules, each labeled with a different color fluorescent dye, were sparsely tethered to the surface of a microscope slide, and the location and identity of each individual molecule were recorded by total internal reflection fluorescence imaging (Fig. S3). Dye-labeled holoenzyme was then introduced into the chamber, and binding was detected by recording the transient appearance of spots of RNAP fluorescence at the positions of the DNA molecules on the surface (Fig. 1*B*). Neither the NtrC activator nor NTPs were added, and therefore, open complex formation and subsequent steps in the initiation pathway did not occur (7, 30). Experiments were conducted in a buffer designed to mimic physiological ionic conditions.

Binding of holoenzyme was observed on both the promoter and nonpromoter DNAs (Fig. 1*C*). Binding to the nonpromoter DNA may represent sequence-independent association of σ^{54}RNAP, analogous to nonpromoter binding seen previously for σ^{70}RNAP (23, 31). Our experiment is not designed to differentiate between molecules bound to a fixed position on the nonpromoter DNA and molecules that may be sliding along the DNA. Nevertheless, binding of RNAP to the promoter DNA was much more frequent than binding to the nonpromoter DNA (Fig. 1*D*), suggesting that many of the binding events on the former were formation of specific promoter–holoenzyme complexes. The initial closed complex of σ^{54}RNAP and this promoter, RP_1, dissociates with a time constant of 2.3 s (7), a duration that is easily detected in these experiments (50% detection threshold ~ 0.2–0.5 s) and is consistent with the lifetimes of the majority of the observed spots.

Although the experiments were conducted at subnanomolar holoenzyme concentrations, which complicate reproducible control of free holoenzyme concentration, performing the measurement on two DNAs simultaneously in the same sample allowed accurate comparison of binding rates under identical solution and imaging conditions. We computed the binding rates by measuring the time until the first observed binding event on each DNA molecule (7). Fitting the distributions of these times revealed that binding to the promoter DNA was 10-fold faster than binding to the nonpromoter DNA (Fig. 1*E*). This finding implies that roughly 90% of the events observed on the promoter DNA are promoter-specific binding events.

The observed binding to the nonpromoter DNA (Fig. 1 *D* and *E*, red traces) might represent generic sequence nonspecific binding of the polymerase along the DNA. Alternatively, it could arise from binding to the DNA ends, the dye moiety, or a nonpromoter tight binding site inadvertently included in the sequence (26, 32, 33). To test for these possibilities, we constructed a nested series of promoter-free sequences of various lengths (Fig. S1) and measured the rate of RNAP binding to each of these relative to the rate of RNAP binding to the 825**N** construct (Fig. 2*A*). Within experimental uncertainty, the measured binding rate increased linearly with DNA length. This observation is inconsistent with the interpretation that the observed binding to the nonpromoter DNAs arises from binding to DNA ends, the dye, or a rare, special sequence. Instead, it is consistent with the hypothesis that the observed events represent sequence nonspecific binding along the DNA.

In the FD model, nearly all binding to the promoter occurs through initial binding to a nonpromoter segment of the DNA (Fig. 1*A*). Thus, the model predicts that the rates of binding to the two DNAs in Fig. 1 *B*–*E* should be almost identical. The data in Fig. 1 *D* and *E* seem inconsistent with this prediction.

Rate of Promoter-Specific Binding Is Independent of the Length of Flanking DNA. The results in Figs. 1 and 2 are fully consistent with simple 3D diffusion of RNAP through solution and direct binding to the promoter. As described above, these data seem inconsistent with the predictions of an FD-mediated promoter approach mechanism. However, this argument is not decisive: it could be that numerous sequence nonspecific binding events are occurring

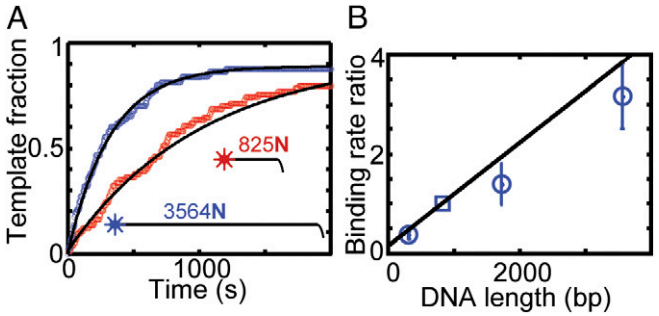

Fig. 2. Binding of σ^{54}RNAP to nonpromoter DNAs of different lengths. (*A*) Comparison (as in Fig. 1*E*) of the rate of 0.3 nM σ^{54}RNAP binding to 3,564- and 825-bp nonpromoter DNAs. Fits (black) give apparent first-order rate constants [blue: $(31 \pm 4) \times 10^{-4}$ s^{-1}, N_D = 81; red: $(10 \pm 2) \times 10^{-4}$ s^{-1}, N_D = 74] yielding a 3564**N**:825**N** binding rate ratio of 3.2 ± 0.7 (SE). (*B*) Relative rate constants for σ^{54}RNAP binding to different length nonpromoter DNAs. Binding rate ratios 306**N**:825**N**, 1735**N**:825**N**, and 3564**N**:825**N** (circles) were measured in comparison experiments (e.g., *A*). Weighted linear fit (black) is constrained such that the 825**N**:825**N** ratio is one (square).

in the experiment in Fig. 1 *B–E* but that these numerous events belong to an additional undetected class of nonspecific binding events. Unlike the measured events (mean lifetime = 4.7 s), this class would have to be too short-lived (i.e., duration << ~0.3 s) (7) to be efficiently detected in our experiments.

To address this concern, we turned to an alternative experimental design that does not require detecting sequence nonspecific binding events. In this design, we varied the length of the DNA segments that flank the promoter, thus changing the size of the target for sequence nonspecific binding. If nonspecific binding to flanking sequences plays a role in finding the promoter, shortening or eliminating the flanking DNA should reduce the rate of promoter binding. An analogous approach was used to study the role of FD in the binding of transcription factors and restriction enzymes to their target sequences in previous ensemble (34, 35) and single-molecule (36) studies.

σ^{54}RNAP contacts with DNA downstream of the promoter do not extend beyond the base pair that encodes the 5′ nucleotide of the transcript (37, 38). We prepared a promoter-containing DNA 595**P**7 that was truncated just downstream of this point. If binding and sliding over distances >>7 bp is the dominant pathway of promoter search, binding to this DNA is expected to be approximately twofold slower than binding to 597**P**255, because the downstream flanking DNA is absent in the former. This expectation is not met; an experiment that compares the rates of binding to the two DNAs reveals that the rates are indistinguishable within experimental uncertainty (Fig. 3*A*). This result is inconsistent with DNA >>7 bp downstream of the promoter significantly accelerating binding by any mechanism, including by FD.

This experiment observed both binding events in which RNAP interacted with the promoter and binding events in which binding was nonspecific. We also performed an independent analysis that scored only the production of specific promoter–RNAP complexes. We previously showed (7) that binding of σ^{54}RNAP (R) to the promoter (P) initially forms a kinetically unstable closed complex (RP_1), which then isomerizes into a much more kinetically stable closed complex (RP_2) (Fig. 3*B*). RP_2 is the precursor to open complex formation and subsequent RNA synthesis. In the experiments reported here, open complex formation is blocked, because activator and NTPs are absent. Thus, dwell time distributions of σ^{54}RNAP bound to DNAs containing the *glnAp2* promoter have two components (Fig. 3*C*), a short component (a combination of RP_1 and nonpromoter binding) and a >10-fold longer promoter-specific component (from complexes that make one or more sojourns into RP_2) (7). Essentially no long-lived (>~10 s) complexes are seen on nonpromoter DNA (Fig. 3*D*, *Inset*). Therefore, the frequency with which long-lived complexes form is proportional to the rate of promoter binding, provided that the efficiency of forming RP_2 from RP_1, $k_2/(k_2 + k_{-1})$ (Fig. 3*B*), is a constant. The frequencies of these long-lived complexes observed on the original and downstream-truncated DNAs were essentially identical (Fig. 3*C*), indicating that the downstream segment does not increase the rate of promoter binding. Thus, the results in Fig. 3 *A* and *C* exclude the possibility that there are sequence nonspecific complexes that form more than 7 bp away from the promoter that significantly accelerate promoter finding by σ^{54}RNAP, even if such postulated complexes have lifetimes too short to be detected in our experiments.

The forgoing results strongly argue that FD over distances longer than ~10 bp is not involved in promoter binding or plays only an undetectably small role on the DNAs <1 kbp in length studied in Figs. 1 and 3 *A* and *C*. We next examined whether FD might start to play a role in at least a minority of promoter binding events when the DNA was longer and sequence nonspecific binding therefore would be more frequent (Fig. 2*B*). When ~3,000 bp of downstream DNA was added to the template, a significant increase in the total number of binding events was observed. However, essentially all of the increase was caused by short-lived binding events, and roughly the same increase was seen regardless of whether the DNA contained a promoter (Fig. 3*D*, *Inset*). Thus, the increment in short-lived events likely arose only from an increase in nonspecific binding. Despite the increase in the total number of binding events, the frequency of long-lived events with and without the downstream extension (Fig. 3*D* and Fig. S5) was

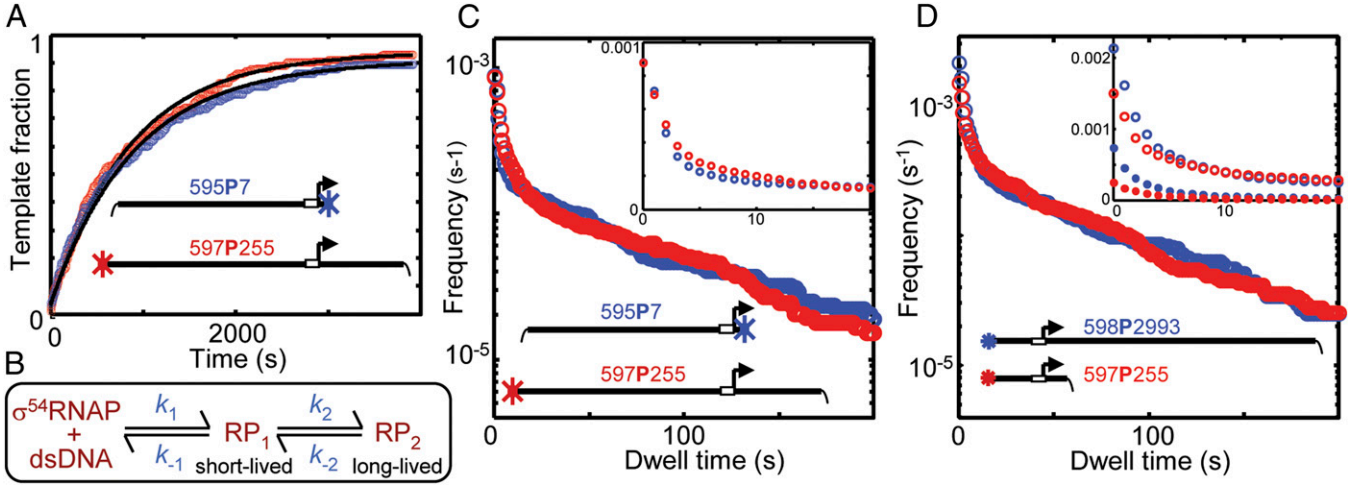

Fig. 3. Binding and dissociation of 0.1 nM σ^{54}RNAP from promoters with different lengths of flanking DNA. (*A*) Comparison of binding rates (as in Fig. 1*E*) to DNAs with 7 and 255 bp downstream of the promoter. The 595**P**7:597**P**255 binding rate ratio 0.95 ± 0.14 (N_D = 189 and 202, respectively) indicates that the rates are the same within experimental uncertainty. (*B*) Kinetic scheme for closed complex formation by σ^{54}RNAP at *glnAp2* from ref. 7. (*C*) Observation frequency of RNAP–DNA complexes with lifetimes greater than or equal to the indicated dwell time on DNAs with a truncated downstream flanking sequence (blue: 595**P**7, number of complexes N_C = 663) or a control (red: 597**P**255, N_C = 735) taken from the same dataset as *A*. (*Inset*) Magnified view plotted on a linear scale of the short dwell time regime. (*D*) Same as *C*, except for a DNA with an extended downstream segment (blue: 598**P**2993, N_D = 122, N_C = 1,000) and control (red: 597**P**255, N_D = 147, N_C = 885). Filled symbols in *Inset* are from a separate experiment on DNAs of similar lengths that lacked the promoter (blue: 3564**N**, N_D = 148, N_C = 2,245; red: 825**N**, N_D = 147, N_C = 1,091) measured at 0.4 nM σ^{54}RNAP and normalized to 0.1 nM. The points at dwell time 0 yield total binding event frequency differences between the long and short DNAs of (6.38 ± 1.32) × 10^{-4} s^{-1} with promoter and (4.92 ± 0.35) × 10^{-4} s^{-1} without promoter.

identical to the limit of experimental uncertainty. Thus, adding the long extension does not detectably increase promoter binding; the data imply that no more than 8% of the long-lived promoter binding events on the long DNA could arise from sliding that originated in the long downstream segment (*SI Materials and Methods*).

A previous study suggested that truncation of segments upstream or downstream had differing effects on promoter occupancy by σ^{70}RNAP (20). In our earlier work (7), we truncated the DNA upstream of the *glnAp2* promoter (instead of downstream) and measured the effects of the truncation on the kinetics of σ^{54}RNAP binding and release using the same methods as in Fig. 3 *A* and *C*. In the upstream-truncated construct, we retained 78 bp of DNA upstream of the transcription start site to avoid removing core promoter and upstream promoter elements that may participate in RNAP promoter binding (39). The experiments (figure s4 a and b in ref. 7) showed clearly that truncation of the upstream DNA from 597 to 78 bp has no detectable effect on the association rate of RNAP with the DNA; k_1 (Fig. 3*B*) is unchanged. Interestingly, truncation of the upstream segment at −78 significantly increases the rate of dissociation (k_{-1}) of the short-lived RP_1 complex while not perturbing k_2 and k_{-2}. Thus, the truncation lowers the efficiency $k_2/(k_2 + k_{-1})$, decreasing the rate at which long-lived complexes are formed, despite the unaltered RNAP-promoter association rate. These observations are consistent with the hypothesis that contact with looped or wrapped DNA farther upstream than −78 helps prevent polymerase dissociation after it arrives at the promoter. Nevertheless, both the upstream and downstream truncation experiments show that sequences outside of the promoter region do not appreciably accelerate promoter binding by σ^{54}RNAP.

Nonspecific Complexes and the Initial Closed Complex Have Similar Kinetic Stabilities. The data in Fig. 1*E* show that, for a promoter-containing DNA of 853 bp, binding of RNAP to the promoter is much faster than its binding to all of the flanking DNA taken together. This effect is even more pronounced for shorter DNAs, because they present a smaller target for nonspecific binding (Fig. 2). Even if we consider only the short component of the dwell time distribution, almost all (~93%) of the binding events to 78**P**255 come from binding to the promoter rather than the flanking DNA (Fig. 4, *Inset*). Significantly, the initial slopes of the dwell time distributions of the RNAP–promoter complexes and complexes on nonpromoter DNA are similar in magnitude (Fig. 4). Taken together, these observations imply that the kinetic stability of the initial complex formed by sequence-specific binding to the promoter is comparable with the kinetic stability of the nonspecific DNA–RNAP complexes that we observe.

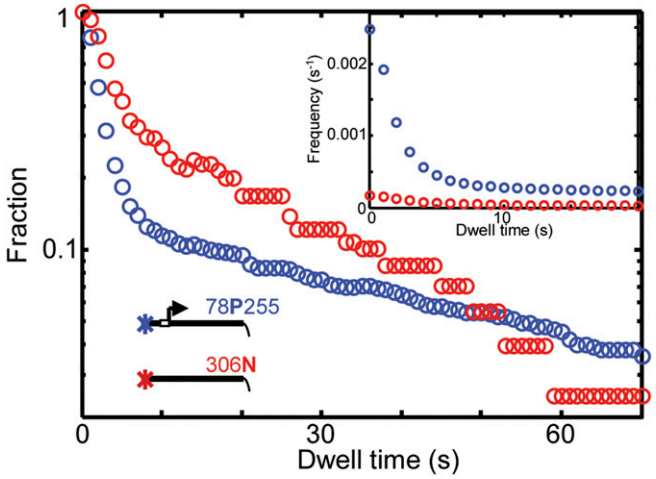

Fig. 4. Fraction of observed RNAP complexes with lifetimes greater than or equal to the indicated dwell time on short DNAs with (blue: 78P255, $N_D = 95$, $N_C = 996$) or without (red: 306N, $N_D = 90$, $N_C = 103$) a promoter. (*Inset*) Frequency distribution of lifetimes in the range of 0–20 s from the same dataset.

Discussion

The data reported here examine whether FD plays a significant role in the binding of σ^{54}RNAP to a promoter using three independent experimental tests. First, the frequency at which RNAP molecules are observed to bind to nonpromoter DNA up to 3.5 kbp in length is too low for those binding events to be intermediates on the pathway by which RNAP reaches the promoter. Second, truncating the DNA flanking a promoter site (down to 78 bp on the upstream side or down to 7 bp on the downstream side) does not substantially reduce the overall RNAP binding rate, implying that flanking DNA segments longer than 7 bp do not play a major role in helping RNAP to reach the promoter. Third, the rate of formation of the long-lived promoter-specific complexes that are known to be obligate intermediates on the initiation pathway also is not affected by changing the length of flanking DNA, confirming that the flanking DNA does not accelerate formation of the promoter complexes relevant to transcription initiation. Taken together, these results exclude FD over distances in the range from ~10 bp to 3 kbp as a significant pathway for σ^{54}RNAP to reach the promoter under the ionic conditions studied here, which are intended to mimic the conditions in live bacteria. They also exclude other mechanisms that use the flanking DNA in this length range (40).

The overall rate of nonspecific binding to a DNA molecule increases as the DNA is lengthened, and the deduced affinity of σ^{54}RNAP for nonpromoter DNA is similar to the nonpromoter affinity previously measured for σ^{70}RNAP (*SI Materials and Methods*). For a promoter embedded in the bacterial genome where the flanking DNA length is >>3 kb, the rate of nonspecific binding might increase to the point where FD could conceivably begin to make at least some significant contribution to the rate at which RNAP reaches the promoter. However, such long distance sliding is unlikely: based on the known size of σ^{54}RNAP and the geometry of the closed complex, we estimate a maximal 1D diffusion coefficient of 1×10^6 bp^2/s (*SI Materials and Methods*). This value implies that, during the mean 4.7 s dwell time that we measure, a nonspecifically bound RNAP can be efficiently captured only if the promoter is located <2,200 bp away from its starting position. However, FD over distances up to 3 kb is excluded by the data already described. Thus, the data exclude sequence nonspecific binding followed by 1D sliding as a mechanism for accelerating promoter binding even in extremely long DNAs.

Our data do not exclude the possibility that FD plays some role in very small-scale RNAP movements that occur after RNAP already partially overlaps the ~30-bp promoter. However, it is likely that these very final movements of RNAP in forming a sequence-specific promoter complex cannot be adequately understood in terms of either FD or 3D diffusion/binding models, both of which treat RNAP as a rigid body moving relative to the DNA (see Introduction). Conversely, our data do not exclude sliding if the efficiency of promoter capture by sliding RNAP is very low, but in this limit sliding would not accelerate promoter binding.

Even proteins that are capable of FD may switch above a facilitation threshold protein concentration to a regime in which search instead occurs primarily by 3D diffusion and direct binding (23). Our experiments were conducted far below this concentration threshold (which is ≥10 nM based on our measurements) (*SI Materials and Methods*). Thus, our data suggest that σ^{54}RNAP does not reach the promoter by FD, even in the low concentration regime. At the higher free σ^{54}RNAP concentrations inferred to be present in living cells (*SI Materials and Methods*), a role for an FD-mediated promoter search is even less likely.

Thus, our data largely exclude the FD mechanism for acceleration of promoter binding shown in Fig. 1*A*. Instead, they are consistent with a simple, one-step binding process, in which RNAP reaches the promoter by 3D diffusion through solution ending in direct, sequence-dependent binding. Therefore, σ^{54}RNAP reaches its target sequence by a mechanism that differs from the mechanism used by the transcription factors and DNA binding proteins that have been observed to reach their targets by sliding (41–43). Many previous studies on *E. coli* RNAP have been interpreted as supporting an FD model for promoter search with sliding distances of hundreds to thousands of base pairs (13–21). Those studies used a different holoenzyme (σ^{70} instead of σ^{54}), and many were conducted at unphysiologically low ionic strength; therefore, it is possible that promoter search by FD occurs under the conditions of those experiments but not our experiments. However, we note that none of the studies show by direct observation that sliding on DNA precedes capture by the promoter, and they do not directly show that sliding increases the net rate at which polymerase reaches the promoter. In contrast to the previous studies, the work reported here directly tests both of these hypotheses and finds neither to be true.

In a recent study, Wang et al. (23) used stretched-out DNA "curtains" on which it was possible to directly visualize sliding of other proteins (e.g., Lac repressor) (23). Wang et al. (23) were unable to directly observe whether nonspecifically bound σ^{70}RNAP (in contrast to σ^{54}RNAP used here) can slide on DNA, because the nonspecific σ^{70}RNAP complexes were too short-lived. However, the short lifetime is incompatible with sliding over thousands of base pairs and thus, seems inconsistent with some earlier observations of long-range sliding of nonspecifically bound σ^{70}RNAP (13). Instead, they inferred from an observed nonlinearity in binding rate dependence on RNAP concentration that FD dominates the σ^{70}RNAP promoter search below ~0.5 nM RNAP but that the size of the DNA target over which FD occurs is small (6 bp). The target size conclusion is based on a rigid-body model for RNAP diffusion, which as discussed above may not be accurate on short distance scales. Nevertheless, the general picture that σ^{70}RNAP promoter search does not involve FD, except possibly at very short distance scales, parallels our σ^{54}RNAP results.

The second-order rate constant for σ^{54}RNAP binding to the promoter, $k_1 = 2.1 \times 10^7\ M^{-1}s^{-1}$ (7), is only ~50-fold slower than the estimated upper limit for the rate of 3D diffusion followed by direct binding (*SI Materials and Methods*). Instead of FD, the experimental results suggest that the RNAP–promoter pair is highly refined to allow rapid direct binding. This refinement is illustrated by the deduced energy landscapes for sequence-specific and nonspecific binding (Fig. 5). Our data show that the initial promoter-specific complex RP_1 and the nonspecific complex have roughly similar dissociation rates (Fig. 4). Thus, the activation free energies for the dissociation processes ($\Delta G^{\ddagger}_{r,N}$ and $\Delta G^{\ddagger}_{r,P}$ in Fig. 5) are comparable. In contrast, the data show that the binding rate constants (corresponding to activation energies $\Delta G^{\ddagger}_{f,N}$ and $\Delta G^{\ddagger}_{f,P}$ in Fig. 5) are profoundly different for nonspecific vs. promoter binding. Indeed, extrapolation of the data in Fig. 2*B* indicates that a nonpromoter DNA would have to be ~7.2 kbp long for the rate of the detected nonspecific binding to equal the rate of binding to a single promoter site (*SI Materials and Methods*). This striking observation is consistent with a mechanism in which the promoter sequence has unusual structural or dynamic features, such that a conformation of DNA favored by the polymerase is highly populated at promoters but only rarely populated in generic DNA. In this context, it is interesting to note that σ^{54} promoters have a characteristic region rich in adenosine/thymidine (A/T) content upstream of the promoter (27), and this particular promoter is also 100% A/T from −11 to +1 relative to the transcription start site. It is possible that these segments of unusual base composition impart atypical structural or dynamic properties to the promoter sequence.

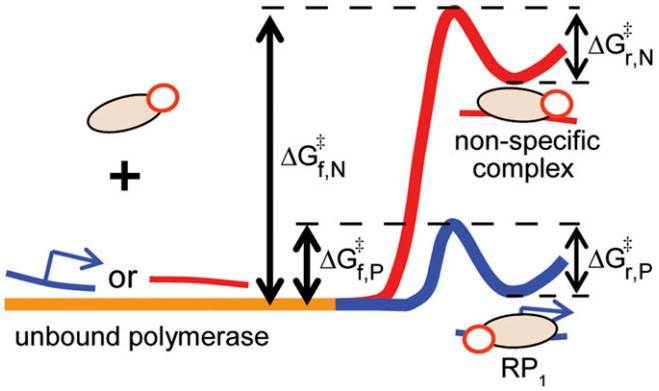

Fig. 5. Schematic free energy landscapes for RNAP binding to a promoter (blue) or a nonspecific site (red) under the conditions of our experiments. Symbols are the same as Fig. 1*A*.

At all transcription promoters, the assumption that the transcription machinery finds promoters by FD has long been problematic, because the presence of other bound proteins on DNA would be expected to impede the sliding search (step 2 in Fig. 1*A*). In bacteria, DNA is occupied by a variety of nucleoid proteins, whereas in eukaryotes, nucleosomes may be positioned flanking, if not at, active promoters (44, 45). In all organisms, DNA in the vicinity of promoters contains binding sites for general and/or specific transcription factors, many of which sites are populated even when the promoter is activated. Our findings of rapid, direct binding of RNAP to promoter DNA and the nonparticipation of the flanking DNA in the promoter-finding process may reflect evolutionary refinement of the RNAP–promoter pair that allows RNAP to find promoters quickly unimpeded by the occupation of the flanking DNA by other bound proteins.

Materials and Methods

Materials. DNA molecules were prepared by PCR as described (7) using the indicated templates and primers (Figs. S1 and S2 and Tables S1 and S2). Nonpromoter DNAs are deleted from −27 to −1 relative to the transcription start site to remove the consensus promoter −12 and −24 sequences.

Core RNAP was obtained from Epicentre. Expression, purification, and dye labeling for the single Cys mutant of σ^{54} and reconstitution of the Cy3-σ^{54}RNAP holoenzyme have been previously described (7). Activity of the holoenzyme was verified using both single-molecule and bulk transcription assays as described previously (7). During a typical single-molecule experiment, the rate of RNAP binding to surface-tethered DNA molecules with an unoccupied promoter declined by only ~7% over 1,000 s, indicating only a small decrease in active, free holoenzyme concentration during the experiments. This minimal decrease is expected based on the slow dissociation of σ^{54}RNAP (46) and is too small to significantly affect the measured rates of association with DNA, particularly because we measure only the relative rates of binding to two DNA molecules in the same sample. In a control experiment, the rate of DNA binding by σ^{54} alone (i.e., without core RNAP) was <0.1% of the rate of binding by holoenzyme.

Microscopy. Measurements were performed using a custom-built multiwavelength micromirror total internal reflection fluorescence microscope equipped with excitation lasers at 633, 532, and 488 nm and a 785-nm laser for autofocus (7, 47).

Flow cells were constructed using fused silica or glass slides passivated with a PEG/biotin-PEG mixture essentially as described (47). The reagents used for this coating were mPEG-SG2000 and biotin-PEG-SVA5000 (Laysan Bio). PEG-coated slides were prepared in advance and stored in a nitrogen atmosphere at −80 °C for up to 6 mo.

All RNAP binding experiments were conducted using a transcription buffer containing 50 mM Tris·OAc, pH 8.0, 100 mM KOAc, 8 mM MgOAc, 27 mM NH_4OAc, 2 mM DTT, 35 mg/mL PEG 8000 (#81268; Sigma-Aldrich), 0.1 mg/mL BSA (#126615; EMD Chemicals), and a glucose/glucose oxidase/catalase oxygen scavenging system to minimize photobleaching (7). This buffer was

also used during the initial attachment of DNA to the flow cell surface, except that PEG was not added until satisfactory surface density of DNA molecules was achieved, because it was found to interfere with DNA attachment to the surface. The interference may be caused by the solution PEG inducing multivalent attachment of streptavidin to the biotin-PEG on the slide surface.

Tethering to the flow cell surface of two types of dye-DNA-biotin molecules, one labeled with Cy5 (Cy5-DNA) and one labeled with Alexa Fluor 488 (AF488-DNA), was performed sequentially. The flow cell was first incubated for 45 s with 0.013 mg/mL streptavidin (Pierce) in transcription buffer lacking both the PEG and oxygen scavenger. The cell was then flushed twice with five times the cell volume using the same buffer followed by a solution containing 10–20 pM AF488-DNA in the same buffer. The accumulation of fluorescent spots from surface attachment of AF488-DNA molecules was monitored to prevent overpopulating the surface and halted by flushing the lane clear with buffer. A solution containing 10–20 pM Cy5-DNA was then added to the lane in transcription buffer lacking PEG but containing oxygen scavenger, and again, the accumulation was halted typically within a few minutes. The microscope stage was then moved to a new field of view (not subjected to prior laser excitation). The instrument was allowed to equilibrate for several minutes to minimize subsequent spatial drift. Next, feedback from the 785-nm IR laser was used to focus the microscope at the new stage position without the photobleaching of the DNA dye labels that would be caused by exposure to visible wavelength excitation. After recording DNA images for a few seconds each using 633- and 488-nm excitation, we commenced the binding measurement by introducing Cy3-σ^{54}RNAP at the specified concentration in transcription buffer. The same DNA imaging was then repeated followed by continuous imaging of the RNAP using 532-nm excitation at a frame rate of 1 s^{-1}, interrupted for ~1 s every ~2 min for automatic focusing.

Methods for analysis of the microscopy data are given in *SI Materials and Methods*.

ACKNOWLEDGMENTS. We thank Jane Kondev for helpful discussion and comments on the manuscript. This work was supported by National Institutes of Health Grant R01 GM 81648 and a grant from the G. Harold & Leila Y. Mathers Foundation.

1. Vannini A, Cramer P (2012) Conservation between the RNA polymerase I, II, and III transcription initiation machineries. *Mol Cell* 45(4):439–446.
2. Saecker RM, Record MT, Jr., Dehaseth PL (2011) Mechanism of bacterial transcription initiation: RNA polymerase - promoter binding, isomerization to initiation-competent open complexes, and initiation of RNA synthesis. *J Mol Biol* 412(5):754–771.
3. Lee DJ, Minchin SD, Busby SJW (2012) Activating transcription in bacteria. *Annu Rev Microbiol* 66:125–152.
4. Gruber TM, Gross CA (2003) Multiple sigma subunits and the partitioning of bacterial transcription space. *Annu Rev Microbiol* 57:441–466.
5. Haugen SP, Ross W, Gourse RL (2008) Advances in bacterial promoter recognition and its control by factors that do not bind DNA. *Nat Rev Microbiol* 6(7):507–519.
6. Roe J-H, Burgess RR, Record MT, Jr. (1984) Kinetics and mechanism of the interaction of Escherichia coli RNA polymerase with the λ PR promoter. *J Mol Biol* 176(4):495–522.
7. Friedman LJ, Gelles J (2012) Mechanism of transcription initiation at an activator-dependent promoter defined by single-molecule observation. *Cell* 148(4):679–689.
8. Bujard H, et al. (1982) *Promoters: Structure and Function*, eds Rodriguez RL, Chamberlin MJ (Praeger, New York), pp 121–140.
9. Halford SE (2009) An end to 40 years of mistakes in DNA-protein association kinetics? *Biochem Soc Trans* 37(Pt 2):343–348.
10. Bai L, Santangelo TJ, Wang MD (2006) Single-molecule analysis of RNA polymerase transcription. *Annu Rev Biophys Biomol Struct* 35:343–360.
11. Wang F, Greene EC (2011) Single-molecule studies of transcription: From one RNA polymerase at a time to the gene expression profile of a cell. *J Mol Biol* 412(5): 814–831.
12. Berg OG, Winter RB, von Hippel PH (1981) Diffusion-driven mechanisms of protein translocation on nucleic acids. 1. Models and theory. *Biochemistry* 20(24):6929–6948.
13. Kabata H, et al. (1993) Visualization of single molecules of RNA polymerase sliding along DNA. *Science* 262(5139):1561–1563.
14. Park CS, Hillel Z, Wu CW (1982) Molecular mechanism of promoter selection in gene transcription. I. Development of a rapid mixing-photocrosslinking technique to study the kinetics of Escherichia coli RNA polymerase binding to T7 DNA. *J Biol Chem* 257(12):6944–6949.
15. Park CS, Wu FY, Wu CW (1982) Molecular mechanism of promoter selection in gene transcription. II. Kinetic evidence for promoter search by a one-dimensional diffusion of RNA polymerase molecule along the DNA template. *J Biol Chem* 257(12): 6950–6956.
16. Singer P, Wu CW (1987) Promoter search by Escherichia coli RNA polymerase on a circular DNA template. *J Biol Chem* 262(29):14178–14189.
17. Singer PT, Wu CW (1988) Kinetics of promoter search by Escherichia coli RNA polymerase. Effects of monovalent and divalent cations and temperature. *J Biol Chem* 263(9):4208–4214.
18. Guthold M, et al. (1999) Direct observation of one-dimensional diffusion and transcription by Escherichia coli RNA polymerase. *Biophys J* 77(4):2284–2294.
19. Harada Y, et al. (1999) Single-molecule imaging of RNA polymerase-DNA interactions in real time. *Biophys J* 76(2):709–715.
20. Ricchetti M, Metzger W, Heumann H (1988) One-dimensional diffusion of Escherichia coli DNA-dependent RNA polymerase: A mechanism to facilitate promoter location. *Proc Natl Acad Sci USA* 85(13):4610–4614.
21. Sakata-Sogawa K, Shimamoto N (2004) RNA polymerase can track a DNA groove during promoter search. *Proc Natl Acad Sci USA* 101(41):14731–14735.
22. Lohman TM (1986) Kinetics of protein-nucleic acid interactions: Use of salt effects to probe mechanisms of interaction. *CRC Crit Rev Biochem* 19(3):191–245.
23. Wang F, et al. (2013) The promoter-search mechanism of Escherichia coli RNA polymerase is dominated by three-dimensional diffusion. *Nat Struct Mol Biol* 20(2): 174–181.
24. Haugen SP, et al. (2006) rRNA promoter regulation by nonoptimal binding of sigma region 1.2: An additional recognition element for RNA polymerase. *Cell* 125(6): 1069–1082.
25. Koo B-M, Rhodius VA, Nonaka G, deHaseth PL, Gross CA (2009) Reduced capacity of alternative sigmas to melt promoters ensures stringent promoter recognition. *Genes Dev* 23(20):2426–2436.
26. Melançon P, Burgess RR, Record MT, Jr. (1982) Nitrocellulose filter binding studies of the interactions of Escherichia coli RNA polymerase holoenzyme with deoxyribonucleic acid restriction fragments: Evidence for multiple classes of nonpromoter interactions, some of which display promoter-like properties. *Biochemistry* 21(18): 4318–4331.
27. Reitzer L, Schneider BL (2001) Metabolic context and possible physiological themes of σ(54)-dependent genes in Escherichia coli. *Microbiol Mol Biol Rev* 65(3):422–444.
28. Wigneshweraraj S, et al. (2008) Modus operandi of the bacterial RNA polymerase containing the σ54 promoter-specificity factor. *Mol Microbiol* 68(3):538–546.
29. Bush M, Dixon R (2012) The role of bacterial enhancer binding proteins as specialized activators of σ54-dependent transcription. *Microbiol Mol Biol Rev* 76(3):497–529.
30. Popham DL, Szeto D, Keener J, Kustu S (1989) Function of a bacterial activator protein that binds to transcriptional enhancers. *Science* 243(4891):629–635.
31. deHaseth PL, Lohman TM, Burgess RR, Record MT, Jr. (1978) Nonspecific interactions of Escherichia coli RNA polymerase with native and denatured DNA: Differences in the binding behavior of core and holoenzyme. *Biochemistry* 17(9):1612–1622.
32. Melançon P, Burgess RR, Record MT, Jr. (1983) Direct evidence for the preferential binding of Escherichia coli RNA polymerase holoenzyme to the ends of deoxyribonucleic acid restriction fragments. *Biochemistry* 22(22):5169–5176.
33. Sanchez A, Osborne ML, Friedman LJ, Kondev J, Gelles J (2011) Mechanism of transcriptional repression at a bacterial promoter by analysis of single molecules. *EMBO J* 30(19):3940–3946.
34. Berg OG, von Hippel PH (1985) Diffusion-controlled macromolecular interactions. *Annu Rev Biophys Biophys Chem* 14:131–160.
35. Jack WE, Terry BJ, Modrich P (1982) Involvement of outside DNA sequences in the major kinetic path by which EcoRI endonuclease locates and leaves its recognition sequence. *Proc Natl Acad Sci USA* 79(13):4010–4014.
36. Wang Y, Guo L, Golding I, Cox EC, Ong NP (2009) Quantitative transcription factor binding kinetics at the single-molecule level. *Biophys J* 96(2):609–620.
37. Burrows PC, Wigneshweraraj SR, Buck M (2008) Protein-DNA interactions that govern AAA+ activator-dependent bacterial transcription initiation. *J Mol Biol* 375(1):43–58.
38. Sasse-Dwight S, Gralla JD (1988) Probing the Escherichia coli glnALG upstream activation mechanism in vivo. *Proc Natl Acad Sci USA* 85(23):8934–8938.
39. Gourse RL, Ross W, Gaal T (2000) UPs and downs in bacterial transcription initiation: The role of the alpha subunit of RNA polymerase in promoter recognition. *Mol Microbiol* 37(4):687–695.
40. Tafvizi A, Mirny LA, van Oijen AM (2011) Dancing on DNA: Kinetic aspects of search processes on DNA. *ChemPhysChem* 12(8):1481–1489.
41. Blainey PC, van Oijen AM, Banerjee A, Verdine GL, Xie XS (2006) A base-excision DNA-repair protein finds intrahelical lesion bases by fast sliding in contact with DNA. *Proc Natl Acad Sci USA* 103(15):5752–5757.
42. Gorman J, et al. (2012) Single-molecule imaging reveals target-search mechanisms during DNA mismatch repair. *Proc Natl Acad Sci USA* 109(45):E3074–E3083.
43. Hammar P, et al. (2012) The lac repressor displays facilitated diffusion in living cells. *Science* 336(6088):1595–1598.
44. Li B, Carey M, Workman JL (2007) The role of chromatin during transcription. *Cell* 128(4):707–719.
45. Jiang C, Pugh BF (2009) Nucleosome positioning and gene regulation: Advances through genomics. *Nat Rev Genet* 10(3):161–172.
46. Maeda H, Fujita N, Ishihama A (2000) Competition among seven Escherichia coli σ subunits: Relative binding affinities to the core RNA polymerase. *Nucleic Acids Res* 28(18):3497–3503.
47. Friedman LJ, Chung J, Gelles J (2006) Viewing dynamic assembly of molecular complexes by multi-wavelength single-molecule fluorescence. *Biophys J* 91(3):1023–1031.